Available online at www.sciencedirect.com
SCIENCE DIRECT
ACADEMIC PRESS
Journal of Sound and Vibration 261 (2003) 527–555
JOURNAL OF SOUND AND VIBRATION
www.elsevier.com/locate/jsvi

Modelling and characterization of airborne noise sources

Yu.I. Bobrovnitskii[a,*,1], G. Pavic[b]

[a] Laboratory of Structural Acoustics, Mechanical Engineering Research Institute of Russian Academy of Sciences, 4M.Kharitonievsky Str., 101990 Moscow, Russia
[b] Laboratoire Vibrations-Acoustique, INSA-Lyon, 20 Avenue Albert Einstein, 69621 Villeurbanne, France

Received 13 August 2001; accepted 8 May 2002

Abstract

A comprehensive model of an arbitrary airborne noise source is developed in this paper. It can be used for noise prediction in complex environment conditions. The model, described by a limited number of parameters—the source impedance and blocked pressure—is invariant with respect to the surrounding acoustical environment. Procedures for experimental identification of model parameters in an arbitrary enclosure are presented. These procedures require only conventional equipment and facilities, and thus can be applied widely. Two analytical examples confirm the validity of the approach.

1. Introduction

The paper deals with modelling and characterization, in frequency domain, of industrial sources of airborne noise, such as machines, equipment, home appliances, etc. Models of these sources are needed for the prediction of the noise levels in rooms, for acoustic design and evaluation of acoustic performance. Characterization is necessary for comparing sources against each other. Since sound generation mechanisms in industrial sources are often too complicated to be adequately described by the available means of analysis (though there are some promising results — see, e.g., Refs. [1,2]), formal or behavioristic source models are commonly used for prediction purposes. Formal models, giving no insight into physics of the internal noise generation, provide approximate mathematical description of the sound field created by the source. To be of practical value, an acoustic source model should be characterized by a limited

*Corresponding author. Tel.: 7-095-1358070; fax: 7-095-1354074.
E-mail address: bobrovni@orc.ru (Yu.I. Bobrovnitskii).
[1] The work has been carried out during the author's visit to Laboratoire de Vibration et Acoustique, INSA-Lyon, France.

doi:10.1016/S0022-460X(02)00981-1

number of parameters that may be easily identified experimentally or numerically. Ideally, these parameters should be invariant with respect to the acoustic load, i.e., independent of the environmental acoustic conditions.

Among the existing formal models of airborne noise sources, the simplest and most often used is the model characterized by a single parameter—the total radiated sound power. The model is employed at high frequencies (where the sound wavelength λ is much smaller than the source dimension l, $\lambda \ll l$) in the prediction methods based on the energy balance equations, SEA in particular [3].

At the other end of the acoustic frequency range ($\lambda \gg l$), i.e., at infrasound and low audio frequencies, the models are also very simple: according to general theory [4], a noise source, as a vibrating body, behaves like and is modeled by a point source—a monopole, a dipole, a quadrupole, or a combination of these.

In the middle frequency range ($\lambda \sim l$), which is of the greatest importance in machinery acoustics and to which the present work is oriented, there are a lot of source models each having its specific field of applicability.

Perhaps, the best of the mid-frequency models and the most popular one is the model represented by the normal velocity distribution over the source outer surface or, in a discretized form, by a set of M normal velocity amplitudes at M points of the surface. These model parameters can be identified by direct measurement as well as indirectly by the acoustic holography techniques [5–7]. When the values of these parameters are available, the sound field of the source can be computed by the boundary element method [8] using, e.g., one of the commercially available code packages [9,10]. The model is applicable to industrial noise sources with casings of high impedance and of simple geometry. If the source casing is made of thin walled, hence resilient, elements, the vibratory velocity amplitudes on such an element in one room would not necessarily be the same in another room, and the model is not invariant with the acoustic environment. Examples of application to designing machine members can be found, e.g., in Refs. [11–13]. However, the model cannot be applied to sources with fluid dynamic effects, like fans, and it is hardly applicable to sources with a complex surface geometry.

There is a big group of mid-frequency formal source models that are composed of a finite number of elementary (point) sources. The modelling elementary sources may be placed inside the real source surface [14–16], or on this surface [17,18], or outside it [19–21]. The model parameters, i.e., the strengths of the elementary sources, are found via matching the actual (measured) and modelling field quantities at a number of points. All these models are very simple and easily handled, but unfortunately they are not invariant with the acoustic environment: values of the model parameters depend equally on the source and room properties unless special measures are not taken as in Ref. [22]. For that reason, the point-source models cannot be used for characterization of airborne noise sources. However, they are very useful in situations when it is required to describe the sound field of a particular industrial source of noise in a particular acoustic environment. Besides, their range of applicability is very large: practically any real source such as a machine can be modelled by a set of point sources.

One more group of models has been developed for fluid machines, such as fans, compressors, pumps and internal combustion engine exhaust systems [2,23–25].

These models are based on the approach used in electric circuit theory: in analogy with the well-known two-port electric source model, an acoustic source model is characterized in the frequency domain by two parameters—the blocked pressure and the internal source impedance. The model is invariant with respect to external load. There are several methods for experimental identification of the model parameters.

This model has been widely and successfully used for prediction of noise in pipe systems and for design of mufflers. It should be noted, however, that the model describes "one-dimensional" sources that are acoustically loaded by one-dimensional structures, like fluid-filled pipes and ducts at not very high frequencies when the plane wave is the only propagating mode in such waveguides. That is why the direct analogy with electric circuits becomes possible here and the model of acoustic sources has only two parameters (fans having the inlet and outlet sides are described by a little more complex four-port source model with three internal impedances). Note that references cited above are only a small part selected by the authors from the vast literature on acoustic sources. For more details of the existing source models see, e.g., Refs. [2,25,26].

A new model of airborne industrial noise source is proposed in this paper. It combines the advantages of the above-mentioned models and avoids most of their disadvantages: extending further the electro-acoustic source analogy to the multi-dimensional case, the proposed model, like the models of fluid machines, is invariant with the acoustic environment and, like the point-source models, has a wide field of applications. It can therefore be used for prediction of the noise levels in rooms as well as for characterization of industrial noise sources.

The present paper is theoretical. It is limited to development of the mathematical and physical basis of the proposed source model and of the accompanying method for noise prediction. Two simple academic examples are presented to validate the general approach. As for the experimental implementation of the method and its application to real noise sources, together with analysis of errors, robustness, and similar questions, they are left for a study to follow.

The layout of the paper is the following. In Section 2, the proposed source model is defined and the corresponding technique for noise prediction is presented. Several procedures are described in Section 3 for experimental identification of the main source and room model parameters. Two analytical examples are presented in Section 4. Section 5 contains remarks on choosing some "free" model parameters. Characterization of airborne noise sources is briefly discussed in Section 6. In Section 7, the main results of the paper are summarized.

2. Source model and its parameters

2.1. Background

The proposed model of an airborne noise source is based on the following theorem on representation of vibro-acoustic fields in linear mechanical systems [27]: the global field in a system composed of two subsystems, one excited and one passive, connected through an interface surface S, can be represented as the sum of two simpler field components. The first component is the field in the isolated subsystems with the interface surface blocked, i.e., with the normal particle velocity on S set to zero. The second component is the forced vibrations of the coupled subsystems under the sole action of the blocked pressure of the first component. To illustrate the main idea of the model, consider a room with an operating machine schematically shown in Fig. 1(a). It is supposed that the machine is perfectly isolated from the supporting structure, so

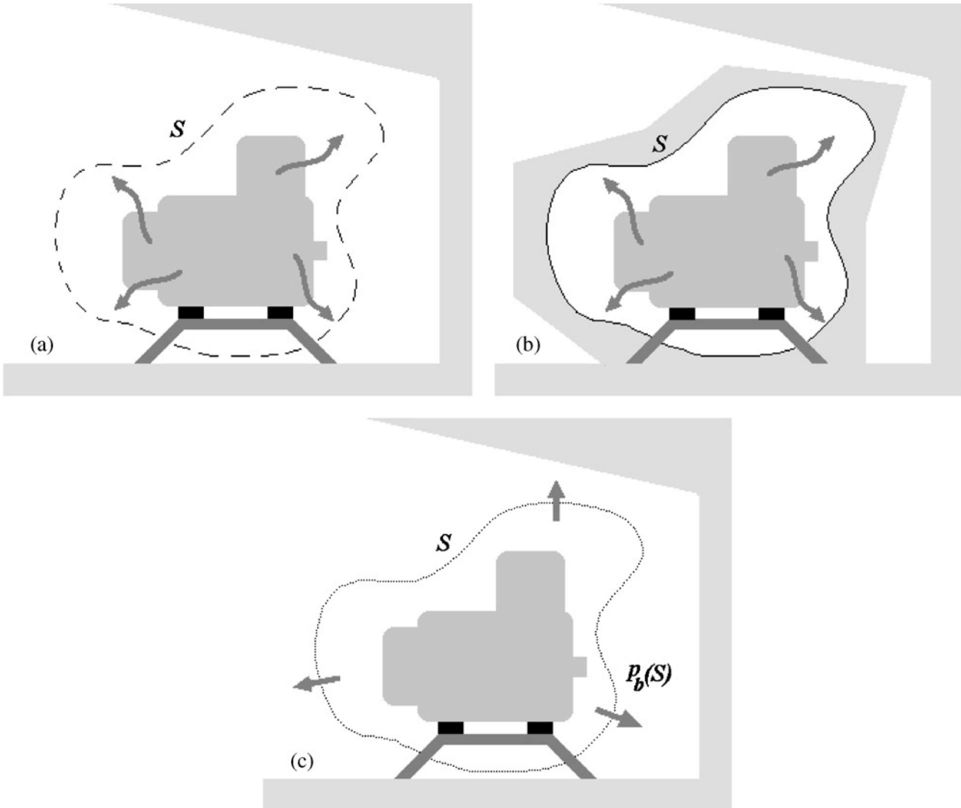

Fig. 1. Characteristic concepts used in the source modelling approach: (a) operating source in its environment (room), S being a virtual enveloping surface; (b) operating source inside the blocked surface S; (c) acoustic field excited by the external distributed force $p_b(s)$ acting on S with the source switched off.

that noise in the room is caused by sound radiation from the machine only. Let S be a surface fully enveloping the machine. Then the system "room/machine" can be considered as composed of two subsystems—the interior of the surface S, i.e., the fluid cavity with the machine inside, and the exterior of S, i.e., the room with the cavity removed. Apply now the above-mentioned theorem to this system. The acoustic pressure field $p(x)$ in the system caused by the operating machine, Fig. 1(a), can be represented as the sum of two components, p_0 and p_1, such that $p(x) = p_0(x) + p_1(x)$, x being an arbitrary point within the system. The first component, $p_0(x)$, is the field of the operating machine with the blocked surface S; see Fig. 1(b). As the machine is the only source in the system, the field in the space exterior to the blocked surface S, is then equal to zero, $p_{0R}(x) = 0$. Inside the blocked surface S the first component is, of course, non-zero, $p_{0S}(x) \neq 0$. The second component $p_1(x)$ is the field in the system with the idle machine caused by the pressure jump across S equal to the blocked pressure applied to S, $p_b(s)$, $s \in S$; see Fig. 1(c). The blocked pressure $p_b(s)$ is equal, according to the theorem, to the first component acting on S, $p_b(s) = p_{0S}(s)$. From this it follows that the acoustic field in the room caused by the operating machine outside S is exactly equal to the field produced by the external distributed force $b(s)$ applied in the normal direction to the surface S enveloping the idle machine and equal to the blocked pressure,

$b(s) = p_b(s)$. It is easy to show that when such a force is applied to S the difference between the pressure amplitudes on two side of S is equal just to the amplitude $b(s)$ at all points of S—see Section 2.5. This force can also be interpreted as a double layer with the source surface density $b(s)$, $s \in S$ [28].

Thus, the original, primary noise source, the operating machine, can be replaced by an equivalent secondary noise source characterized by the enveloping control surface S and by the excitation force $b(s)$. The source model proposed in this paper is, in fact, this secondary source somewhat simplified for the sake of its effective identification. The rigorous definition of the model is given in the next Section 2.2. It is worth noting that the replacement of the primary source by the secondary one makes noise prediction and source characterization much easier. First of all, the separation of a source/room system into two subsystems by means of an enveloping control surface (which may stay the same for different noise sources and rooms) allows one to characterize independently sources and rooms and employ a unified approach to wide classes of noise sources and acoustic environments. Besides, as shown in Section 3, the room and sources parameters may, in this case, be identified experimentally. The replacement of a primary noise source by the proposed secondary one also means that the physical sources of sound radiation are transferred in the model from the outer source surface, often of very complex geometry, to a much simpler control surface S. This allows one to take advantage of some well elaborated techniques, e.g., the one based on spherical functions. For the sake of convenience, the control surface S enveloping a noise source is taken further in this paper as a spherical one. However, the basic results remain valid when other types of the control surface are used, e.g., a box-like surface.

2.2. Definition of the source model

The proposed model of airborne noise source is reduced from the secondary source of spherical geometry introduced in the previous subsection. In this case, all the field quantities can be expanded in spherical functions retaining a limited number of terms. The following two assumptions are made at this point. First, only N first spherical harmonics are taken into account for the construction of the excitation force $b(s)$ distributed on the spherical surface S. The second assumption concerns the way the fluid within the sphere containing the idle source is taken into account. It is represented by an impedance-type $N \times N$-matrix defined with respect to N spherical components of the external force acting on S. This implies in turn that the internal acoustic field within the sphere is described on S by the N spherical harmonics only. Consider these assumptions in more detail.

Since spherical harmonics constitute on a spherical surface a complete set of functions, the blocked pressure and, hence, the excitation force $b(s)$, can be expanded in these functions as

$$p_b(s) = p_b(\varphi, \theta) = \sum_{n=0}^{\infty} \sum_{m=0}^{n} [b_{nm}^c Y_{nm}^c(\varphi, \theta) + b_{nm}^s Y_{nm}^s(\varphi, \theta)] = b(s), \quad (1)$$

where Y_{nm}^c and Y_{nm}^s are the normalized spherical harmonics [29], and b_{nm}^c and b_{nm}^s are the amplitudes of these harmonics. The first assumption requires the blocked pressure to be sufficiently accurately described by the lowest N spherical harmonics and therefore may be characterized by N parameters—the amplitudes of the spherical harmonics in Eq. (1) arranged in an N-sized vector

$$\boldsymbol{b} = [b^c_{00}, b^c_{10}, \ldots, b^c_{nl,nl}]^{\mathrm{T}}. \tag{2}$$

The number N is related to the largest harmonic order $n = nl$. If the spherical harmonics of orders $n = 0, 1, \ldots, nl$ are taken into account in expansion (1), the number N, i.e., the size of the vector (2), is generally equal to $N = nl^2 + 1$. Practically, it may be reduced, e.g., by symmetry of the problem as in the examples of Section 4. Note that the amplitudes b^s_{n0}, $n \neq 0$, do not appear in Eq. (2) since the corresponding spherical functions are zero functions. Physically, the first assumption means that when a noise source is operating inside the blocked spherical surface S the variation of the blocked pressure on S is smooth enough. How to choose the number N is discussed in Section 5.

According to the second assumption, the passive secondary spherical source, i.e. the fluid-filled cavity containing the idle noise source is fully described by a $N \times N$-matrix $\boldsymbol{Z_S}$ of source impedances. Alternatively, an equivalent representation of the cavity by a mobility matrix $\boldsymbol{Y_S} = \boldsymbol{Z_S^{-1}}$ is possible too. Either of the two refers to an external force distributed across S. The two representations are defined by the equations

$$\boldsymbol{f} = \boldsymbol{Z_S u}, \quad \boldsymbol{u} = \boldsymbol{Y_S f}, \tag{3}$$

where $\boldsymbol{f} = [f^c_{00,} \ldots]^{\mathrm{T}}$ is the N-sized vector of type (2) composed of N spherical amplitudes of an external force $f(s)$ applied in the normal positive direction to S, and $\boldsymbol{u} = [u^c_{00,} \ldots]^{\mathrm{T}}$ is a similar N-sized vector of the secondary source radial velocity response on S. Physically, the second assumption means that the field of the passive secondary source due to an external force composed of the first N spherical harmonics will contain only N essential spherical components.

The definition of the impedance matrix and mobility matrix in Eq. (3), relating the coefficients of expansion in spherical functions of the force and velocity response, differs from the traditional definition of the impedances and mobilities that relate directly the force and velocity amplitudes [30]. A physical sense of the element $(\boldsymbol{Y_S})_{ij}$ is the following: it represents the amplitude of the ith spherical harmonic of the velocity response to the external pressure in the form of the jth spherical harmonic of unit amplitude. Similar physical sense has the source impedance matrix: if the vibration velocity of the surface S is prescribed in the form of the kth spherical harmonic of unit amplitude, the amplitude of the jth spherical harmonic of the internal pressure at S is equal to $(\boldsymbol{Z_S})_{jk}$.

By combining the two assumptions, the following definition of the model of airborne noise sources can be formulated: the model, Fig. 2(a), is a sphere S of radius a characterized by the $N \times N$-matrix of the source surface impedances (3); excitation in the model is provided by the N-vector (2) of the external force applied to the surface S and equal to the blocked pressure. The model, thus, contains $1 + N(N+1)/2$ scalar parameters: radius a of the enveloping sphere; number N of the blocked pressure components $\boldsymbol{b}$; $N(N-1)/2$ different components of the source impedance matrix $\boldsymbol{Z_S}$ (which is complex and symmetric).

This model can be interpreted as an extension to the multi-dimensional case of the one-dimensional electric source model, characterized by the electromotive force and internal resistance. The blocked pressure components and the source internal impedances have to be determined experimentally—see Section 3. Radius a and number N are chosen depending on the type of noise source and frequency range under study—see Section 5.

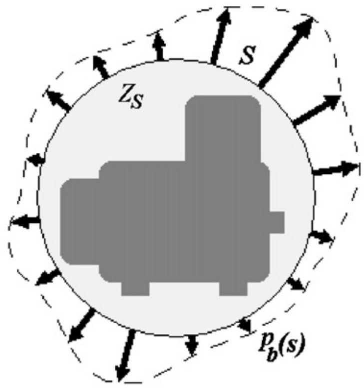

(a)

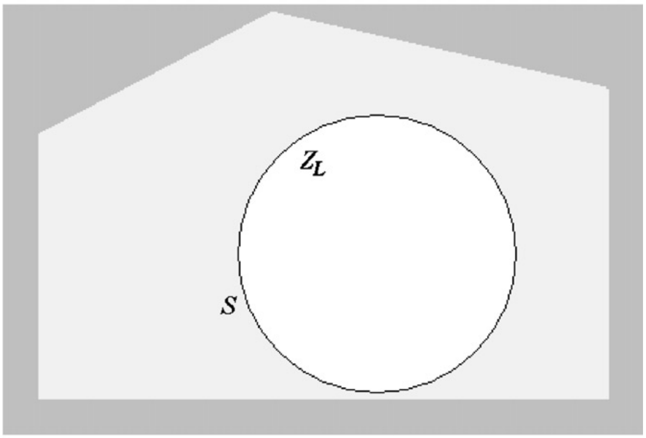

(b)

Fig. 2. Elements of sound prediction procedure: (a) acoustic source model—a fluid-filled spherical cavity containing the source structure, characterized on S by the matrix of source impedances Z_S and the blocked pressure $p_b(s)$, (b) model of the source environment (room) exterior to S, characterized by the matrix of room impedances Z_L.

2.3. Model invariance with acoustic environment

The source model defined above is invariant with the acoustic environment. To prove the statement, it is sufficient to show that the model parameters have the same values in various rooms.

Consider a sound source in two different rooms. Let the control surface S and the number N of the spherical harmonics be the same for both rooms. Now apply the theorem [27] to these two cases. It is evident that the blocked pressures and, hence, the blocked pressure vectors are identical in both cases, since they are not influenced by the room properties when the source and room are isolated by the blocked control surface. So are the matrices of the source impedances: they are determined only by the source, independently of the room. Thus, all the source model parameters are the same for the two different rooms and thus the model is invariant with the acoustic environment.

The invariance does not mean that the casing and other outer elements of a noise source should have invariant amplitudes of vibration. On the contrary, resilient thin-walled elements may have different vibrational amplitudes in different environmental conditions. This is provided for in the matrix of the source impedances. At the same time, the sound generation processes inside the source, such as unbalance, impacts, etc., are assumed to be the same in any acoustic environment. Also, the acoustic properties of the surrounding fluid (air) are assumed identical in all cases.

2.4. Room model and its parameters

The main objective of modelling is the prediction of the noise levels in complex acoustic environments. Any prediction technique uses a certain model of a noise source as well as a model of a room. Both models must fit each other and be of the same order of accuracy. The room model which matches the above defined source model is shown in Fig. 2(b). It represents the exterior of the spherical control surface S. Being the acoustic load of the source, the room model is assumed to be represented by $N \times N$-matrix $\boldsymbol{Z_L}$ of the room impedances (i.e., acoustic load impedances) or by its inverse $\boldsymbol{Y_L}$, the room mobility matrix, similar to the source matrices $\boldsymbol{Z_S}$ and $\boldsymbol{Y_S}$. A physical meaning of this assumption is the same as that of the second assumption for the source model (see Section 2.2): if an external force $g(s)$ acting on S in normal direction consists of no more than N first spherical harmonics, the response $v(s)$ of the room, i.e., the radial velocity component on S, is also constituted of no more than N spherical harmonics, with the amplitudes of harmonics higher than the Nth assumed negligible. Inversely, if on the control surface S the radial velocity distribution is prescribed in the form of N first spherical harmonics, the pressure field in the room on S does not contain more than N spherical components. The size N of the room impedance matrix depends on geometry and acoustic properties of the room, damping in particular, as well as on the number of essential harmonics in the source model—see Section 5.

Thus, the room model is characterized by $1 + N(N-1)/2$ scalar parameters: radius a of the sphere and the symmetric matrix $\boldsymbol{Z_L}$ of the room impedances containing $N(N-1)/2$ elements. The main equations that describe the room field are similar to those for the source model (3):

$$\boldsymbol{g} = \boldsymbol{Z_L v}, \quad \boldsymbol{v} = \boldsymbol{Y_L g}, \tag{4}$$

where $\boldsymbol{g} = [g_{00}^c, \ldots]^{\mathrm{T}}$ is an N-vector composed of the first N coefficients of expansion of the type (1) for an external force $g(s)$ applied to S, while $\boldsymbol{v} = [v_{00}^c, \ldots]^{\mathrm{T}}$ is a similar N-vector of the room velocity response $v(s)$ at S.

2.5. Source/room coupled field

Now suppose that the parameters of the model of a noise source and the model parameters of a room are available and it is required to predict the sound field in the room. The radius of the sphere S and number N of spherical harmonics are taken the same for both models. To find the sound field in the room means to compute the amplitudes of the coupled vibrations of the source model and the room model, connected continuously on the spherical surface S, under the action of external force $b(s)$ distributed on S and equal to the blocked pressure (see Section 2.1).

Two boundary conditions must be satisfied on S. First, the radial velocity $u(s)$ of the source model should be equal to the radial velocity $v(s)$ of the room model at each point $s \in S$, $u(s) = v(s)$. And second, the sum of the force $f(s)$ acting at S on the source model and the force $g(s)$ acting at S on the room model should be equal to the external force $b(s)$, $f(s) + g(s) = b(s)$. Since $f(s) = p_{1S}(s)$, $g(s) = -p_{1R}(s)$, and $b(s) = p_b(s)$, this condition also means that the difference between the pressures at the inner and outer sides of S must be equal to the blocked pressure $p_b(s)$, $p_{1S}(s) - p_{1R}(s) = p_b(s)$.

After expanding these velocities and forces in the spherical harmonics and retaining the first N essential spherical coefficients, these two boundary conditions at S can be represented in equivalent vector form via the expansion coefficients as

$$\boldsymbol{u} = \boldsymbol{v}, \quad \boldsymbol{f} + \boldsymbol{g} = \boldsymbol{b}, \tag{5}$$

where $\boldsymbol{b}$ is the blocked pressure vector of size N. Other N-vectors are defined in Eqs. (3) and (4). Substitution of Eqs. (3) and (4) into Eq. (5) yields the following solution for the coupled field of the room/source system via the impedance model parameters:

$$\begin{aligned} \boldsymbol{u} = \boldsymbol{v} &= (\boldsymbol{Z_S} + \boldsymbol{Z_L})^{-1}\boldsymbol{b}, \\ \boldsymbol{f} &= \boldsymbol{Z_S}(\boldsymbol{Z_S} + \boldsymbol{Z_L})^{-1}\boldsymbol{b}, \\ \boldsymbol{g} &= \boldsymbol{Z_L}(\boldsymbol{Z_S} + \boldsymbol{Z_L})^{-1}\boldsymbol{b} \end{aligned} \tag{6}$$

and via the mobility model parameters

$$\begin{aligned} \boldsymbol{u} = \boldsymbol{v} &= \boldsymbol{Y_S}(\boldsymbol{Y_S} + \boldsymbol{Y_L})^{-1}\boldsymbol{Y_L}\boldsymbol{b} = \boldsymbol{Y_L}(\boldsymbol{Y_S} + \boldsymbol{Y_L})^{-1}\boldsymbol{Y_S}\boldsymbol{b}, \\ \boldsymbol{f} &= (\boldsymbol{Y_S} + \boldsymbol{Y_L})^{-1}\boldsymbol{Y_L}\boldsymbol{b}, \\ \boldsymbol{g} &= (\boldsymbol{Y_S} + \boldsymbol{Y_L})^{-1}\boldsymbol{Y_S}\boldsymbol{b}. \end{aligned} \tag{7}$$

This solution gives the field quantities of the room, the radial velocity $v(s)$ and the pressure amplitudes $p_{1R}(s) = g(s)$, only on the interface surface S. For practical purposes, this is often sufficient, in particular, when only the power W injected into the room is required. By definition, the power is equal to

$$W = \frac{1}{2}\mathrm{Re}\int_S \overline{v(s)} \cdot g(s)\,\mathrm{d}s,$$

where the bar denotes complex conjugate. When the radial velocity $v(s)$ and the force $g(s)$ are expanded on S in spherical harmonics and substituted into this equation, the power W can be expressed in terms of the matrix model parameters as

$$W = \tfrac{1}{2}\mathrm{Re}(\boldsymbol{v}^*\boldsymbol{g})$$

and after substituting Eq. (6)

$$W = \tfrac{1}{2}\boldsymbol{v}^*\,\mathrm{Re}\boldsymbol{Z_L}\boldsymbol{v} = \tfrac{1}{2}\boldsymbol{b}^*(\boldsymbol{Z}_{\boldsymbol{S}}^* + \boldsymbol{Z}_{\boldsymbol{L}}^*)^{-1}\,\mathrm{Re}\boldsymbol{Z_L}(\boldsymbol{Z_S} + \boldsymbol{Z_L})^{-1}\boldsymbol{b}, \tag{8a}$$

or after using Eq. (7)

$$W = \tfrac{1}{2}\boldsymbol{g}^{*}\,\mathrm{Re}\,\boldsymbol{Y_L g} = \tfrac{1}{2}\boldsymbol{b}^{*}\boldsymbol{Y}_{\boldsymbol{S}}^{*}(\boldsymbol{Y}_{\boldsymbol{S}}^{*} + \boldsymbol{Y}_{\boldsymbol{L}}^{*})^{-1}\,\mathrm{Re}\,\boldsymbol{Y_L}(\boldsymbol{Y_S} + \boldsymbol{Y_L})^{-1}\boldsymbol{Y_S b}, \tag{8b}$$

where the star designates the Hermitian conjugate.

Thus, in the proposed method, the coupled field characteristics of the source/room system are expressed through a limited number of model parameters defined with respect to the control surface. As a result of such an economic description of subsystems, solution (6), (7) omits details of the coupled field giving the field amplitudes on the interface surface only. The necessary details, if needed, can be obtained by the BEM or FEM or transfer function measurement using the boundary values given in Eqs. (6) and (7). Note that Eqs. (4)–(8) are valid not only for a the spherical control surfaces but for a control surface of any geometry.

2.6. A modification of the source model

The blocked pressure vector $\boldsymbol{b}$ is not always the most appropriate parameter of the noise source model defined in Section 2.2. The reason is that it is strongly dependent on the acoustic properties of the cavity between the noise source and the blocked sphere S. At the cavity resonance frequencies, the blocked pressure may be very large and it may also be very small at its antiresonance frequencies. In the acoustic field of the entire source/room system these maxima and minima are not seen, as they are compensated by the source impedances which vary with frequency in the similar manner, Eq. (6). Nevertheless, this filter effect of the source cavity is sometimes undesirable, e.g., when the source model radius a is large, so it is reasonable to replace the blocked pressure by another parameter that depends on frequency more smoothly.

In the modified source model defined in this subsection the blocked pressure $p_b(s)$ is replaced by the pressure $p_\infty(s)$ on surface S when the source radiates into free space. Correspondingly, the blocked pressure vector $\boldsymbol{b}$ is replaced by N-vector $\boldsymbol{p}_\infty$ composed of the first N coefficients of expansion of function $p_\infty(s)$ in spherical harmonics. Other parameters of the source model, i.e., the source impedances and radius a, remain unchanged. Mathematically, the model based on $\boldsymbol{p}_\infty$ is equivalent to that based on $\boldsymbol{b}$ in that the two produce identical results where prediction of sound field created by the source is concerned. Physically, the two models may be slightly different in a certain sense—see Section 5. Below, the main equations for the modified model are presented.

Let $\boldsymbol{Z}_\infty$ be the load impedance matrix of the free space or, more exactly, of the unbounded fluid in the exterior of the spherical surface S of radius a

$$\boldsymbol{Z}_\infty = \begin{bmatrix} Z_{\infty,0} & & & 0 \\ & Z_{\infty,1} & & \\ & & \cdots & \\ 0 & & & Z_{\infty,nl-1} \end{bmatrix} = \mathrm{diag}[Z_{\infty,n}], \quad Z_{\infty,n} = \mathrm{i}\rho c \frac{\mathrm{h}_n(ka)}{\mathrm{h}_n'(ka)}, \tag{9}$$

where h_n is the spherical Hankel function of order n, a prime denotes the derivative, ρc and k are the characteristic impedance and wavenumber of the fluid [29]. Substituting this load impedance into Eq. (6) and taking into account that $g(s) = p_\infty(s)$ on S, one obtains the following equation relating $\boldsymbol{b}$ and $\boldsymbol{p}_\infty$

$$\boldsymbol{p}_\infty = \boldsymbol{Z}_\infty(\boldsymbol{Z_S} + \boldsymbol{Z}_\infty)^{-1}\boldsymbol{b} = (\boldsymbol{Z_S Y}_\infty + \boldsymbol{I})^{-1}\boldsymbol{b}, \tag{10}$$

where $\boldsymbol{Y}_\infty = \boldsymbol{Z}_\infty^{-1}$ and $\boldsymbol{I}$ is the identity matrix. After substituting vector $\boldsymbol{b}$ by its expression in terms of vector $\boldsymbol{p}_\infty$, solution (6) for coupled system vibrations with load $\boldsymbol{Z_L}$ can be rewritten in the form

$$\boldsymbol{u} = \boldsymbol{v} = (\boldsymbol{Z_S} + \boldsymbol{Z_L})^{-1}(\boldsymbol{Z_S}\boldsymbol{Y}_\infty + \boldsymbol{I})\boldsymbol{p}_\infty,$$

$$\boldsymbol{f} = (\boldsymbol{Z_L}\boldsymbol{Y_S} + \boldsymbol{I})^{-1}(\boldsymbol{Z_S}\boldsymbol{Y}_\infty + \boldsymbol{I})\boldsymbol{p}_\infty,$$

$$\boldsymbol{g} = (\boldsymbol{Z_S}\boldsymbol{Y_L} + \boldsymbol{I})^{-1}(\boldsymbol{Z_S}\boldsymbol{Y}_\infty + \boldsymbol{I})\boldsymbol{p}_\infty. \tag{11}$$

Eqs. (7) and (8) for the coupled field and power flow can also be rewritten in the similar manner by using Eq. (10).

3. Model parameter identification

In this section, experimental techniques for the identification of the model parameters are outlined. These techniques do not require any particular facilities and use commercially available instruments. Only general ideas and basic relations are presented below. Technical details of implementation of these techniques will be the subject of a forthcoming publication.

3.1. Identification of the room model parameters

Identification of the room parameters, i.e., the elements of the room impedance $N \times N$-matrix $\boldsymbol{Z_L}$, can be made with the use of N different test sources of small dimension with known blocked pressure vectors $\boldsymbol{b_1}, \ldots, \boldsymbol{b_N}$. The term "different" means in this case that vectors $\boldsymbol{b_j}$ have to be linearly independent. Practically, these test sources can be realized by using, for example, two small loudspeakers oriented in various directions—see Section 3.3. The procedure for identification of the room parameters is depicted in Fig. 3. The kth small test source having the vector $\boldsymbol{b_k}$ is placed inside the interface surface S. When the source is switched on, the complex pressure amplitudes are measured at M grid points of S and then processed so that a N-vector $\boldsymbol{p_k}$ composed of the N first spherical harmonic coefficients of the pressure expansion on S is

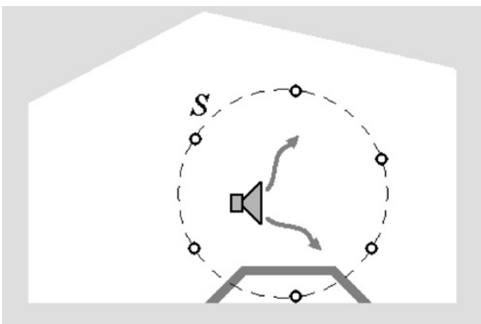

Fig. 3. Experimental procedure for the identification of environmental (room) parameters: a small test source—loudspeaker—emits sound in the room from the interior of the control surface S. The sound pressure is measured by microphones (circles) at grid points of S.

obtained. If j_n is the spherical Bessel function of order n and

$$\boldsymbol{Z}_0 = \mathrm{diag}[Z_{0,n}], \quad Z_{0,n} = -\mathrm{i}\rho c \frac{\mathrm{j}_n(ka)}{\mathrm{j}'_n(ka)}, \quad n = 0, 1, \ldots, nl - 1 \tag{12}$$

is the impedance matrix of the fluid-filled sphere S of radius a (which is equal to the internal impedance matrix of each of the small test sources), then according to Eq. (6) the pressure $\boldsymbol{p_k}$ is equal to

$$\boldsymbol{p_k} = \boldsymbol{g_k} = \boldsymbol{Z_L}(\boldsymbol{Z}_0 + \boldsymbol{Z_L})^{-1}\boldsymbol{b_k}$$

or in another form

$$(\boldsymbol{Z}_0\boldsymbol{Y_L} + \boldsymbol{I})\boldsymbol{p_k} = \boldsymbol{b_k}. \tag{13}$$

Repeating the measurement for N test sources and combining N Eq. (13), $k = 1, 2, \ldots, N$, in one matrix equation

$$(\boldsymbol{Z}_0\boldsymbol{Y_L} + \boldsymbol{I})\boldsymbol{P} = \boldsymbol{B}, \tag{14}$$

where the columns of the $N \times N$-matrices $\boldsymbol{P}$ and $\boldsymbol{B}$ are the vectors $\boldsymbol{p_k}$ and $\boldsymbol{b_k}$, one can derive from this equation the needed load matrix of the room mobilities

$$\boldsymbol{Y_L} = \boldsymbol{Y}_0(\boldsymbol{B}\boldsymbol{P}^{-1} - \boldsymbol{I}), \tag{15a}$$

where $\boldsymbol{Y_L} = \boldsymbol{Z_L^{-1}}$, $\boldsymbol{Y_0} = \boldsymbol{Z_0^{-1}}$, $\boldsymbol{I}$ is the identity matrix. If the number N_1 of the test sources is greater than the number N of the essential spherical harmonics, $N_1 > N$, matrices $\boldsymbol{P}$ and $\boldsymbol{B}$ are rectangular having N_1 rows and N columns. The solution of Eq. (14) in this case can be obtained by the least mean square technique as

$$\boldsymbol{Y_L} = \boldsymbol{Y_0}[\boldsymbol{B}\boldsymbol{P}^*(\boldsymbol{P}\boldsymbol{P}^*)^{-1} - \boldsymbol{I}]. \tag{15b}$$

Solution (15b) is less affected by the measurement errors and, thus, is more robust than solution (15a).

3.2. Identification of the source parameters

Two methods for identification of the source model parameters are described below. One permits one to measure directly all the source parameters but at the cost of designing and manufacturing a special spherical "camera" (chamber). Another method, similar to that described in Section 3.1, allows one to identify the source parameters in arbitrary room but indirectly, i.e., through measurement and matrix computations of type (15).

3.2.1. Rigid spherical camera

In this method, a noise source under study is placed inside a spherical camera with a rigid wall and with the inner radius a equal to that of the control surface S (Fig. 4). When the source operates, the microphones inserted into the wall at grid points of S measure directly the blocked pressure on the rigid wall. After expanding the pressure in spherical harmonics, one obtains the source parameter $\boldsymbol{b}$. The source impedance matrix $\boldsymbol{Z_S}$ can be measured in the camera also directly, if the source is idle and the actuators (e.g., ceramic plates regularly placed on S) provide the radial velocity distribution on S in the form of, say, kth spherical harmonic. Then the pressure measured

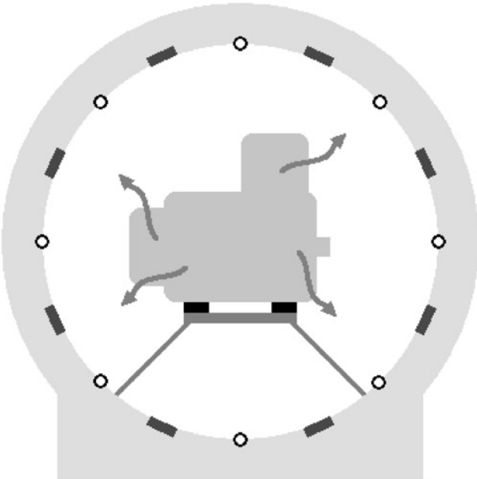

Fig. 4. Spherical camera of rigid walls for direct measurement of source model parameters. Microphones (circles) and sound actuators (bars) are flush mounted in the wall at regularly spaced grid points.

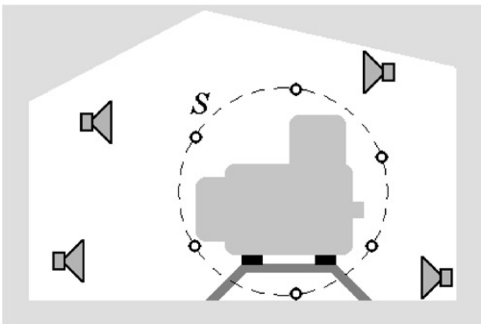

Fig. 5. Identification of source model parameters in an arbitrary enclosure. Test sources—loudspeakers—are located outside the control surface S. The sound pressure is measured at grid points of S by microphones (circles).

by the microphones on S and expanded into spherical harmonics with coefficients $\boldsymbol{p}_k$ gives directly the kth column of the sought matrix $\boldsymbol{Z}_S$.

The method of a rigid spherical camera is very attractive since it allows one to measure directly all the source model parameters. However, its implementation is not simple. Besides, some sources, e.g., fans, cannot normally operate in such conditions. To these sources, the following method can be applied.

3.2.2. *Identification in arbitrary room*

The source parameters may be identified in an arbitrary room with the help of $N_2 > N$ different test sources located outside surface S, see Fig. 5. It is assumed that the room impedance matrix $\boldsymbol{Z}_R$ is already measured by the method of Section 3.1 and the blocked pressure vectors $\boldsymbol{b}_m$ of the outer test sources are known. (Note that the room driven by the mth outer test source may be regarded as an active subsystem (source) with blocked pressure vectors $\boldsymbol{b}_m$ and impedance matrix $\boldsymbol{Z}_R$.) The procedure for identification of the source parameters is the following. First the source mobility matrix $\boldsymbol{Y_S}$ is obtained. For this purpose, the sound is produced by the mth outer test source in the room with the idle noise source, and the pressure amplitudes are measured on S, Fig. 5. According to Eq. (6), the following equation is valid

$$\boldsymbol{b_m} = (\boldsymbol{Z_R}\boldsymbol{Y_S} + \boldsymbol{I})\boldsymbol{p_m}. \tag{16}$$

Repeating the measurement N_2 times for all the outer test sources and combining all Eqs. (16) into one matrix equation,

$$\boldsymbol{B} = (\boldsymbol{Z_R}\boldsymbol{Y_S} + \boldsymbol{I})\boldsymbol{P}, \tag{17}$$

one can find from this equation the mobility matrix of the noise source as

$$\boldsymbol{Y_S} = \boldsymbol{Y_R}[\boldsymbol{B}\boldsymbol{P}^*(\boldsymbol{P}\boldsymbol{P}^*)^{-1} - \boldsymbol{I}]. \tag{18}$$

Here $\boldsymbol{B}$ and $\boldsymbol{P}$ are rectangular $N_2 \times N$—matrices composed of vectors $\boldsymbol{b_m}$ and $\boldsymbol{p_m}$.

The blocked pressure N-vector $\boldsymbol{b}$ of the source under study is identified in the following way. The test sources are switched off, the noise source is set to operate and the complex pressure amplitudes are measured on S. In this case, the room matrix $\boldsymbol{Z_R}$ represents the load impedance matrix of the source, and the sought vector $\boldsymbol{b}$ is obtained from Eq. (6) as

$$\boldsymbol{b} = (\boldsymbol{Z_S}\boldsymbol{Y_R} + \boldsymbol{I})\boldsymbol{p}. \tag{19}$$

3.3. Test sources

The procedures of the model parameter identification described above use, beside ordinary measuring acoustic instruments, a set of the test sources: $N_1 > N$ inner[2] small test sources for identifying the room parameters and $N_2 > N$ outer test sources for the identification of the noise source parameters. This does not mean that $N_1 + N_2$ physically separate acoustic sources are needed. A few ordinary loudspeakers employed in various positions may suffice. This point as well as identification of the test source parameters are discussed below.

3.3.1. Small inner test sources

These sources should be small compared to the wavelength and radius a of the control sphere S. This requirement is needed for neglecting the source dimension and considering the interior of the sphere S with such a source (see Fig. 3) as the fluid-filled ‘‘empty’’ sphere having impedance (12).

Practically, the small test sources can be realized with the help of two or three small loudspeakers as follows. One free loudspeaker (i.e., without a box) provides three different test sources when oriented along three orthogonal axes and producing three independent fields dominantly of the dipole type. Similarly, two closely spaced free loudspeakers, working in phase or anti-phase, can provide nine different test sources giving three fields of the nearly dipole type and six independent fields almost of the quadrupole type (an example of such a loudspeaker pair is described in Ref. [31]). Thus, one loudspeaker in a small box (having non-zero volumetric velocity and generating a field of the near monopole type) and two closely spaced free loudspeakers can provide ten different linearly independent fields that are sufficient for identifying 10×10-matrices

[2] The terms ‘‘inner’’ and ‘‘outer’’ refer to the control surface S.

of the room impedances (N=10). It should be emphasized that the proposed method does not require that the test sources were of the pure monopole, dipole or quadrupole type; the main condition is independence of their blocked pressure vectors.

By rotating the loudspeakers over various space angles one may obtain other acoustic fields and, thus, increase the number N_1 of the inner test sources. These fields, however, are linearly dependent on the main fields. They cannot increase the number of the identified room model parameters, but can prove useful for suppressing the measurement errors.

In general case, when the number N_1 of the small inner test sources (not necessarily loudspeakers) and the number N of the spherical harmonics retained in the expansions are large, the maximum number of the room parameters that may actually be identified is determined by the rank of matrices $\boldsymbol{P}$ and $\boldsymbol{B}$ of the measured pressure amplitudes in Eqs. (14) and (15).

As for the model parameters of the small test sources, the blocked pressure vectors $\boldsymbol{b_k}$ can be measured directly in the rigid walled camera (see Section 3.2.1). Another way is to measure the free space pressure vector $\boldsymbol{p}_\infty$ in an anechoic chamber and obtain $\boldsymbol{b_k}$ from Eq. (10). Because of small dimensions of the test source, its matrix of the internal impedances is assumed to be equal to matrix (12), $\boldsymbol{Z_S} = \boldsymbol{Z_0}$.

3.3.2. Outer test sources

The outer test sources employed in identification of the noise source parameters need not to be of small wave dimension. These may be a set of loudspeakers, free or boxed, located outside the control surface. For example, if the room is of ordinary geometry, e.g., a parallelepiped, six loudspeakers placed at the centroids of the walls, floor and ceiling driven in phase or counter-phase are sufficient for generating at least 10 independent sound fields in the room and, hence, for identifying the parameters of the source model with $N = 10$ essential spherical harmonics. Changing the phases or locations of the loudspeakers one can obtain other test outer sources that can be used for increasing stability of the identification algorithm.

The room outside S with operating the mth outer test source can be regarded as an active subsystem, that is to say as a source with the blocked pressure vector $\boldsymbol{b_m}$ and the source impedance matrix $\boldsymbol{Z_R}$. The unknown vector $\boldsymbol{b_m}$ can be found if this source is loaded by the impedance matrix (12), i.e., by an "empty" fluid-filled sphere S. Switching the mth outer test source on and measuring the pressure amplitudes on S to obtain vector $\boldsymbol{p_m}$ of the spherical coefficients, one derives from Eq. (6) the needed parameters of vector $\boldsymbol{b_m}$,

$$\boldsymbol{b_m} = (\boldsymbol{Z_R Y_0} + \boldsymbol{I})\boldsymbol{p_m}. \tag{20}$$

4. Examples

Two simple academic examples are worked out analytically in this section to validate the proposed approach to modelling airborne sound sources and predicting their acoustic fields in rooms. Two types of noise sources are considered: a source of the Neumann type, i.e., with prescribed kinematic excitation (Example 1), and a source of the Dirichlet type, i.e., with prescribed force excitation (Example 2). In order to make these examples more realistic, the position of the source in Example 1 is shifted with respect to the center of the control sphere, while in Example 2 the size of the source is taken finite. The radiation problems in both examples are simple enough to have exact analytical solutions. Solutions to the problems, based on the proposed models for sources and rooms, are obtained and compared against the exact analytical solutions.

4.1. Example 1: shifted monopole in a sphere

As the first example, consider the acoustic field of a monopole with prescribed volumetric velocity q [m^3s^{-1}] in a spherical chamber. The position of the monopole does not coincide with the chamber center O (chosen as the coordinate origin) and is shifted along the axis Oz at distance l, Fig. 6. The wall of the chamber has a lining with the local impedance Z_w. It is required to find the acoustic field in the chamber using the approach presented in this paper and assess it via comparison with the exact analytical solution.

4.1.1. Analytical solution

The exact analytical solution to the radiation problem shown in Fig. 6 is obtained with the help of the well-known techniques [29] in the form of a series in spherical functions. Omitting the details of derivation, the pressure amplitude at a chamber point with spherical co-ordinates r, θ (Fig. 6) can be written as

$$p_{ex}(r,\theta) = \frac{1}{4\pi}\rho c k^2 q \sum_{n=0}^{\infty} \mathrm{P}_n(\cos\theta)\mathrm{j}_n(kl)\left\{\mathrm{h}_n(kr) - \frac{\delta_n(kR)}{\Delta_n(kR)}\mathrm{j}_n(kr)\right\}, \tag{21}$$

Here ρc and k are the characteristic impedance and wavenumber of the fluid; $\mathrm{P}_n(.)$ is the Lagrange polynomial of the first kind and order n; j_n and h_n are the spherical Bessel and Hankel functions of order n; R is the radius of the chamber; a prime denotes the derivative with respect to

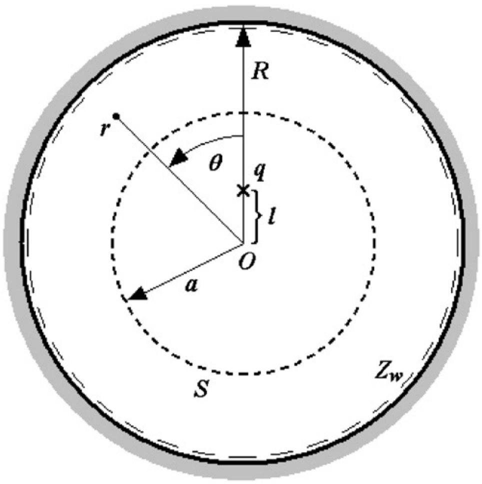

Fig. 6. Example 1: monopole q at a distance l from the centre of a spherical chamber of radius R. The control surface S is a sphere of radius a concentric with the chamber; Z_w is a locally reacting impedance of the chamber wall.

the argument,

$$\delta_n(kR) = \mathrm{h}_n(kR) + \mathrm{i}(Z_w/\rho c)\mathrm{h}'_n(kR),$$

$$\Delta n(kR) = \mathrm{j}_n(kR) + \mathrm{i}(Z_w/\rho c)\mathrm{j}'_n(kR). \tag{22}$$

In general case, the pressure field (21) of the shifted monopole contains spherical functions of all orders describing outgoing waves (h_n) as well as standing waves (j_n). When the eccentricity distance l tends to zero, solution (21) reduces to one term corresponding to the field component of the monopole type, $n = 0$. Equations $\Delta_n(kR) = 0$, $n = 0, 1, \ldots$, are the frequency equations of the chamber. At these frequencies the standing wave components are at maximum. The expression for $\delta_n(kR)$ in Eq. (22) is proportional to the difference between the wall impedance and the free space impedance (9):

$$\delta_n(kR) = \frac{\mathrm{h}'_n(kR)}{\mathrm{i}\rho c}(Z_\infty - Z_w)_n.$$

When the monopole radiates into free space, all δ_n are equal to zero and, applying the addition theorem for spherical functions, solution (21) becomes the well-known classical solution [29]

$$p_{ex}(r, q) = \frac{1}{4\pi}\rho c k^2 q \sum_{n=0}^{\infty} \mathrm{P}_n(\cos\theta)\mathrm{j}_n(kl)\mathrm{h}_n(kr) = \frac{1}{4\pi}\rho c k^2 q \mathrm{h}_0(kr_1), \tag{23}$$

where $r_1 = |\boldsymbol{r} - \boldsymbol{l}|$ is the radius from the monopole position to the observation point.

The power flow W from the source into the chamber is equal to the power dissipated in the wall lining

$$W = \frac{1}{2}\mathrm{Re}\int\int_{S_R} p(R,\theta)\overline{v(R,\theta)}\,\mathrm{d}S = \frac{1}{2}\mathrm{Re}Z_w \int\int_{S_R} |v(R,\theta)|^2\,\mathrm{d}S, \tag{24}$$

where v is the radial velocity complex amplitude; S_R is the spherical wall surface of radius R. Substitution into Eq. (24) of pressure amplitude (21) and/or velocity amplitude $v = (\mathrm{i}\rho\omega)^{-1}\partial p/\partial r$ yields the following equation:

$$W = \frac{1}{8\pi}\rho c k^2 |q|^2 \frac{\mathrm{Re}(Z_w/\rho c)}{(kR)^2} \sum_{n=0}^{\infty} \frac{\mathrm{j}_n^2(kl)}{2n+1}\frac{1}{|\Delta_n|^2}. \tag{25}$$

When the monopole radiates into the free space the power flow is equal to [29]

$$W_\infty = \frac{1}{8\pi}\rho c k^2 |q|^2 \sum_{n=0}^{\infty} \frac{\mathrm{j}_n^2(kl)}{2n+1} = \frac{1}{8\pi}\rho c k^2 |q|^2. \tag{26}$$

It is seen from Eq. (25) that the power injected into the cavity is strongly dependent on the wall impedance Z_w. In particular, when the impedance is pure reactive the radiation power is zero.

4.1.2. Model parameters

The objective now is to obtain a solution to the problem using the approach presented in Section 2. Let S be a spherical control surface of radius a centered at the origin O and enveloping the monopole ($R > a > l$)—see Fig. 6. The exterior of S will be considered as the room (passive) subsystem, and the interior of S is the source (active) subsystem. According to the approach, the source subsystem is replaced by the spherical source model which is characterized by the blocked pressure N-vector $\boldsymbol{b}$ (or, equivalently, by the free space pressure N-vector $\boldsymbol{p}_\infty$) and $N \times N$-matrix $\boldsymbol{Z_S}$ of the source impedances. The room subsystem, representing an acoustic load of the source model, is characterized by $N \times N$-matrix $\boldsymbol{Z_L}$ of the room impedances defined at surface S. Consider these parameters in more detail.

The source impedance matrix is in this case the matrix (12) for the fluid-filled sphere of radius a

$$\mathbf{Z_0} = \mathrm{diag}[Z_{0,n}], \quad Z_{0,n} = -\mathrm{i}\rho c \frac{\mathrm{j}_n(ka)}{\mathrm{j}_n'(ka)}, \quad n = 0, 1, \ldots, N-1. \tag{27}$$

To obtain the excitation vector $\boldsymbol{b}$ of the source, it is necessary to find the acoustic field p_b of the monopole q within the blocked surface S. This field can be derived in a similar manner as the field (21)

$$p_b(r, \theta) = Q \sum_{n=0}^{\infty} \mathrm{P}_n(\cos\theta) \mathrm{j}_n(kl) \left\{ \mathrm{h}_n(kr) - \frac{\mathrm{h}_n'(ka)}{\mathrm{j}_n'(ka)} \mathrm{j}_n(kr) \right\}, \tag{28}$$

where $Q = (1/4\pi)\rho c k^2 q$. Putting $r = a$ one obtains the blocked pressure

$$p_b(a, \theta) = -\frac{\mathrm{i}Q}{(ka)^2} \sum_{n=0}^{\infty} \mathrm{P}_n(\cos\theta) \frac{\mathrm{j}_n(kl)}{\mathrm{j}_n'(ka)} \tag{29}$$

and the blocked pressure N-vector $\boldsymbol{b}$ which consists of the first N components of expansion (29)

$$\boldsymbol{b} = \begin{Bmatrix} b_0 \\ b_1 \\ \\ b_{N-1} \end{Bmatrix} = \{b_n\}, \quad b_n = -\frac{\mathrm{i}Q}{(ka)^2} \sqrt{\frac{S}{2n+1}} \frac{\mathrm{j}_n(kl)}{\mathrm{j}_n'(ka)}. \tag{30}$$

Using Eq. (10), one can also compute the free space pressure vector

$$\boldsymbol{p}_\infty = \{p_{\infty,n}\}, \quad p_{\infty,n} = Q \sqrt{\frac{S}{2n+1}} \mathrm{j}_n(kl) \mathrm{h}_n(ka), \quad n = 0, 1, \ldots, N-1. \tag{31}$$

Here $S = 4\pi a^2$ is the area of the control surface.

For obtaining the load $N \times N$-matrix $\boldsymbol{Z_L}$ of the room subsystem one has to find the acoustic field in the cavity between the boundary sphere S_R and the control sphere S excited by the external force $g(s)$ applied to S. The solution to this problem is readily found in the form of a series in spherical functions from the boundary conditions: $p(a) = g(s)$ and $p(R) - Z_w v(R) = 0$. Since the both spherical boundaries, S and S_R, are concentric and the cavity is, thus, spherically symmetric, the external force $g(s)$ consisting of N first spherical harmonics on S will not excite in the cavity more than these N components:

$$p(r, \theta) = \sum_{n=0}^{N-1} g_n \mathrm{Y}_{n0}^c(\cos\theta) d_n^{-1} \left[h_n(kr) - \frac{\delta_n}{\Delta_n} \mathrm{j}_n(kr) \right], \tag{32}$$

where g_n are the elements of the force vector $\boldsymbol{g}$ representing the amplitudes of the spherical harmonics of the force $g(s)$; δ_n and Δ_n are given in Eq. (22); Y_{n0}^c is a normalized spherical harmonic [29]. Deriving from (32) the radial component of the particle velocity, $v = (\mathrm{i}\rho\omega)^{-1}\partial p/\partial r$, and putting $r = a$, one can obtain the load $N \times N$-matrix which, due to the spherical symmetry, is diagonal:

$$\boldsymbol{Z_L} = \mathrm{diag}[Z_{L,n}], \quad Z_{L,n} = \mathrm{i}\rho c \frac{d_n}{D_n}, \tag{33}$$

where

$$D_n = \mathrm{h}'_n(ka) - \frac{\delta_n}{\Delta_n}\mathrm{j}'_n(ka),$$

$$d_n = \mathrm{h}_n(ka) - \frac{\delta_n}{\Delta_n}\mathrm{j}_n(ka). \tag{34}$$

Equations $D_n = 0$ are the frequency equations of the cavity with the blocked surface S, while equations $d_n = 0$ are the frequency equations of this cavity with the soft surface S.

Once the parameters (27) and (30) or Eq. (31) of the source model and those (33) of the room model have been identified, the coupled field in the chamber can be readily evaluated.

4.1.3. Coupled field

Let the parameters of the source model, i.e., the impedance matrix (27) and the blocked pressure vector (30), as well as the parameters of chamber (33) be known. It is required, using these parameters, to obtain a solution for the coupled field.

Substitution of parameters (27), (30) and (33) into Eqs. (6) gives

$$\boldsymbol{Z_S} + \boldsymbol{Z_L} = \mathrm{diag}[Z_n], \quad Z_n = \frac{\rho c}{(ka)^2}\frac{1}{\mathrm{j}'_n(ka)D_n},$$

$$\boldsymbol{v} = (\boldsymbol{Z_S} + \boldsymbol{Z_L})^{-1}\boldsymbol{b} = \{v_n\}, \quad v_n = -\frac{\mathrm{i}Q}{\rho c}\sqrt{\frac{S}{2n+1}}\mathrm{j}_n(kl)D_n, \tag{35}$$

$$\boldsymbol{g} = \boldsymbol{Z_L}\boldsymbol{v} = \{g_n\}, \quad g_n = Q\sqrt{\frac{S}{2n+1}}\mathrm{j}'_n(kl)d_n,$$

where $n = 0, \ldots, N-1$; D_n and d_n are given in Eqs. (34). Eqs. (35) define the radial velocity and pressure amplitudes of the coupled field on the control surface S. Exactly the same equations can be derived if the free space pressure vector (31) is used instead of the blocked pressure vector (30). To obtain the full pressure field in the chamber one should substitute components (35) of vector $\boldsymbol{g}$ into the solution (32). The sought solution for the pressure field in the chamber is equal to

$$p(r,\theta) = \frac{1}{4\pi}\rho c k^2 q \sum_{n=0}^{N-1} \mathrm{P}_n(\cos\theta)\mathrm{j}_n(kl)\left[\mathrm{h}_n(kr) - \frac{\delta_n}{\Delta_n}\mathrm{j}_n(kr)\right]. \tag{36}$$

Similarly, substituting the velocity and force vectors (35) into Eq. (8) one can obtain the power flow from the source into the chamber

$$W = \frac{1}{8\pi}\rho c k^2 |q|^2 \frac{\mathrm{Re}(Z_w/\rho c)}{(kR)^2}\sum_{n=0}^{N-1}\frac{\mathrm{j}_n^2(kl)}{2n+1}\frac{1}{|\Delta_n|^2}. \tag{37}$$

Comparing solutions (36), (37) with the exact solutions (21), (25), one can see that the difference between them consists of contributions of the spherical components that are not taken into account in the source and room models. The accuracy of the model-based solution depends, thus, on the number N of the spherical harmonics retained in the model, as well as on the chosen criterion of the solution quality, i.e., on the chosen objective of prediction—the power flow into the chamber, the overall total energy, the pressure amplitudes at certain points or averaged over the chamber, at discrete frequencies or in frequency bands, etc.

Suppose that the power flow into the chamber in frequency domain is used as the objective. Fig. 7 presents by dots the exact power flow (25) and by the solid lines the contributions of different spherical components of solution (37). The numbering of the curves indicates the order of spherical harmonic n. The curves in Fig. 7 correspond to the following parameters: the eccentricity of the source position is $l/a = 0.5$; the radius of the chamber is five times the radius of the control surface, $R/a = 5$; the wall impedance is $Z_w/\rho c = 0.3(1 + ka) + i3.0$. It is seen from Fig. 7 that at low frequencies, $ka<1$ i.e., $kR<5$, the power flow into the chamber is fully determined by the first spherical component of the monopole type, $n = 0$. In a more wide range of low and middle frequencies, $ka<5$, which comprises more than 60 eigenfrequencies of the chamber, the two components of the monopole ($n = 0$) and dipole ($n = 1$) types are sufficient for a good estimation of the power injected into the chamber. At high frequencies, $ka > 5$, contribution of spherical components of quadrupole, octopole and higher modes increase and become comparable with that of the monopole and dipole types. But this is already the frequency range of applicability of simple energy prediction methods like SEA, which makes detailed source modeling unnecessary.

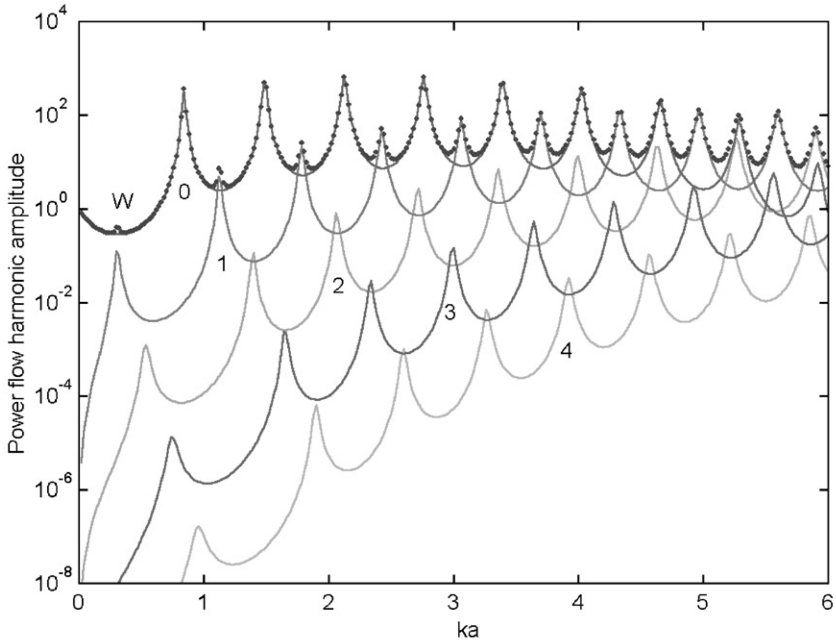

Fig. 7. Power flow W into the chamber (dots) and contributions of the spherical components $n = 0-4$ (thin lines).

4.2. Example 2: forced oscillating rigid ball

As a second example, consider a rigid ball of mass m and radius b oscillating under the action of an external, sinusoidally varying force F, see Fig. 8. This source differs from the one in the first example by its finite size and the nature of excitation which is here a prescribed force rather than a prescribed velocity. The objective of analysis is the same as before, i.e., to check the validity of the prediction method based on the developed room and source models. The validation will be done by comparing the radiation from the source once into free space and then into a chamber, the latter being of the same dimensions and impedance as in Example 1.

To obtain an exact solution to the radiation in free space or into the chamber, one has first to formulate the boundary condition on the surface S_b of the ball. The radial velocity of the oscillating sphere is described by the first order spherical harmonic:

$$v(b,\theta) = v_{max}\cos\theta = v_{max}\mathrm{P}_1(\cos\theta).$$

Here θ is the angle between the radius to the observation point and the direction of oscillation (see Fig. 8), v_{max} being the maximum radial velocity of the ball surface. It is known [29] that such a spherical velocity distribution induces on S_b the pressure of the same distribution pattern, $p(b,\theta) = p_{\max}\mathrm{P}_1(\cos\theta)$. The resultant force acting on the ball is oriented in the direction of oscillation and equals

$$F_z = -\int\int_{S_b} p(\cos\theta)\cos\theta\,\mathrm{d}S_b = -\tfrac{1}{3}p_{max}S_b, \tag{38}$$

the area of the ball surface being equal to $S_b = 4\pi b^2$.

According to the second Newton's law, the equation of motion of the ball is

$$F + F_z = m\mathrm{d}v/\mathrm{d}t,$$

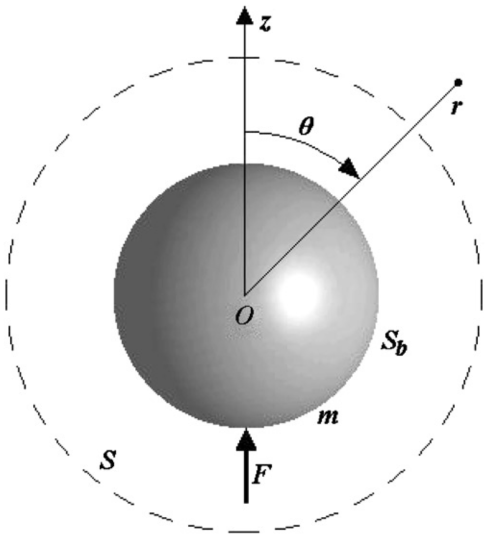

Fig. 8. Example 2: rigid ball of mass m and radius b driven by force F oscillates in the fluid. S is the control surface.

F being the driving force. Upon replacing F_z by the right-hand side of Eq. (38) and equating the velocity of ball oscillation with that of fluid particles at the surface S_b, the equation of motion can be transformed to the needed boundary condition:

$$p_{\max} - \mathrm{i}\rho c k b \mu v_{max} = 3F/S_b, \tag{39}$$

where $\mu = m/M$ represents the ratio of the mass of the ball m and that of the fluid of the same volume as the ball, $M = 4\pi\rho b^3/3$.

The exact analytical solution for the free-field pressure in an arbitrary point at a distance r from the origin is of the form $p(r,\theta) = A\mathrm{P}_1(\cos\theta)\mathrm{h}_1(kr)$. Using the boundary condition (39), one can readily find the unknown coefficient A and, thus, the final expression for the free-field pressure of a force-driven oscillating ball:

$$p_{\text{free}}(r,\theta) = \frac{3F}{S_b}\frac{\mathrm{P}_1(\cos\theta)\mathrm{h}_1(kr)}{\mathrm{h}_1(kb) - \mu kb\mathrm{h}_1'(kb)}. \tag{40}$$

The exact solution for the pressure field of the oscillating ball centred at the origin of a spherical chamber of given wall impedance is somewhat more cumbersome to evaluate. The result is

$$p_{\text{chamber}}(r,\theta) = \frac{3F}{S_b}\mathrm{P}_1(\cos\theta)\frac{\Delta_1\mathrm{h}_1(kr) - \delta_1\mathrm{j}_1(kr)}{\gamma_1\Delta_1 - \delta_1\Gamma_1} \tag{41}$$

with $\gamma_1 = \mathrm{h}_1(kb) - \mu kb\mathrm{h}_1'(kb)$, $\Gamma_1 = \mathrm{j}_1(kb) - \mu kb\mathrm{j}_1'(kb)$, δ_1 and Δ_1 given by Eq. (22). The denominator of Eq. (41) corresponds to the frequency equation of the spherical chamber having a passive ball of mass m in its center. As the source/chamber system is spherically symmetric in this example, the excitation by the oscillating ball produces only a dipole-type response. Therefore, both exact solutions, Eq. (40) for the free field and Eq. (41) for the chamber, contain only one spherical term, that of order $n = 1$.

To obtain the radiated pressure field by the developed modelling method, one should first choose a control surface. A spherical surface S concentric to the source is a natural choice here; see Fig. 8. Then, the active subsystem, i.e., the interior of S containing the ball, and the room subsystem, i.e., the exterior of S, have to be specified in terms of the source and load impedances $\boldsymbol{Z_S}$ and $\boldsymbol{Z_L}$ as well as by the force excitation at the control surface S. Because of spherical symmetry, all the matrices and vectors reduce here to single scalars. The load impedances $\boldsymbol{Z_L}$ for the free-field and chamber are given by Eqs. (9) and (33) after setting $n = 1$. The source parameters may be obtained from Eqs. (40) or (41). As the algebraic manipulations are rather complicated, they all are omitted here. However, the authors have verified that the solutions obtained by the proposed method are precisely equal to the exact solutions (40) and (41).

5. On the choice of the number of harmonics

As was pointed out in Section 3, most of the modal parameters of noise sources and rooms, namely, the impedance matrices $\boldsymbol{Z_S}$ and $\boldsymbol{Z_L}$ as well as the excitation vectors $\boldsymbol{b}$ and $\boldsymbol{p}_\infty$, are determined experimentally. The rest of them—the number N of essential spherical harmonics and the radius a of the control surface, are to be chosen by taking the nature of the source and the room into account. As the number of harmonics is equal to the size of the impedance matrices and to the length of the excitation vectors, a minimum number of these has to exist which provides a given accuracy of the field prediction. In Example 1, the number of spherical harmonics was chosen via comparison of equivalent solution (37) against the exact solution (25)—see Fig. 7. The number is small, $N = 2$ ($n = 0$ and 1), for this academic source/room configuration due to very rapid convergence of series (25): its terms decrease as $n^{-3}(l/R)^{2n}$. For real noise sources with a complicated geometry and shape of vibration, the number of essential harmonics may be noticeably greater. Besides, the exact solutions to the problem are seldom available in practice. How to choose the optimal number N in this general case is briefly discussed below.

According to the basic equations of the proposed method, (6) and (11), the resulting acoustic field in the room represents coupled vibration of the source/room system under the action of the external excitation, the blocked pressure or free space pressure, applied to the control surface S. The noise levels in the room are, hence, determined by the parameters of this excitation and by the properties of the room. Consequently, the number of essential harmonics N in the source model depends on the same parameters as well as on the required accuracy, frequency range and on the objective of prediction. In other words, it depends practically on all the parameters of the problem. However, approximately, this number can be estimated by using limited information: the free space pressure $p_\infty(s)$ of the source on the control surface S and the loss factor of the room where the source is supposed to operate. The idea of the estimation procedure is the following. If, for example, the loss factor is known to be greater than 0.02, then retained in the source model should be all the harmonics the amplitudes of which are greater than 2% of the maximum amplitude. Such a choice makes it likely that the harmonics not taken into account in the source model will not decisively affect the pressure levels in the room even in non-resonant regions of the frequency spectrum. Consider this procedure in more detail and apply it to the source model of Example 1.

Let the objective function of prediction be the power W injected into the room and the loss factor of the room be not less than 0.01 which is the loss factor provided by the wall lining used in Example 1. The contribution W_n of the nth spherical harmonic to the total power is proportional to $p_n v_n$ where p_n is the nth component of the free space pressure vector (10), (31) and v_n is the amplitude of the nth component of the radial velocity on the control surface S. This velocity amplitude is proportional to the pressure component p_n and, according to Eq. (11), inversely proportional to the corresponding room impedance which, in its turn, is proportional to the frequency term Δ_n of the room vibrations—see Eqs. (22), (34), (35). Consequently, the component W_n of the sound power is proportional to the free pressure component square $|p_n|^2$ and inversely proportional to Δ_n of the nth shape of the room vibration, $W_n \propto |p_n|^2/\Delta_n$. This quantity is at maximum at the room resonance frequencies, which correspond to minimum of $|\Delta_n|$, and is proportional to

$$W_n \propto |p_n|^2/\eta. \tag{42}$$

Thus, to estimate the relative contribution W_n of the nth spherical harmonic to the radiated power W, it is sufficient to assess the relative contribution p_n of this harmonic to the free space pressure p_∞ and the loss factor η of the room resonances.

Now apply these estimates to the choice of the optimal number of harmonics in the source model of Example 1. Suppose that are known the room loss factor $\eta \geqslant 0.01$ and the components of the free space pressure vector (31). Fig. 9 shows these components relative to the zero harmonic amplitude, $|p_n/p_0|$ for $n = 0-4$. It is seen in Fig. 9 that at low frequencies, $ka < 1$, the component

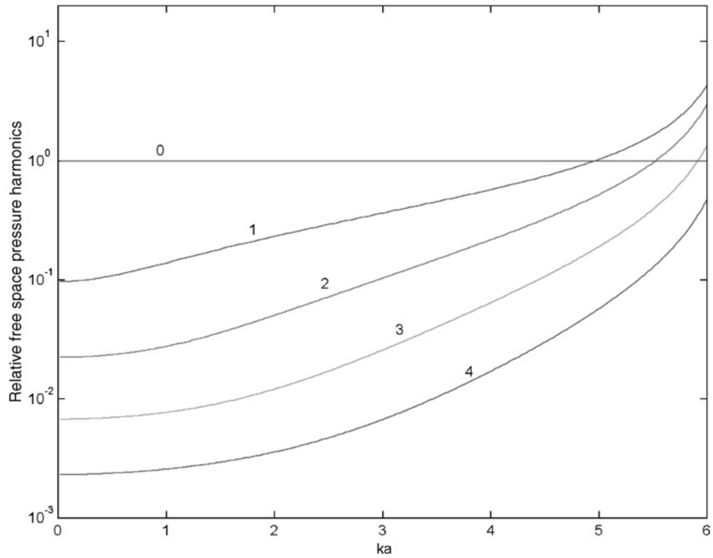

Fig. 9. The free space spherical harmonic amplitudes (31), normalised with the amplitude of the zeroth harmonic, for orders $n = 0-4$. Eccentricity equals to $l/a = 0.5$.

of the monopole type ($n = 0$) is dominant. It exceeds by an order of magnitude the nearest component of the dipole type ($n = 1$). Hence, its contribution to the power flow is two orders of magnitude larger than that of other components at all low frequencies with possible exception of the room resonance of the dipole type where, according to Eq. (42), the contribution of the dipole component may be comparable with that of the monopole component. At higher frequencies, $ka > 1$, the relative contribution of higher harmonics increases. The contribution of the dipole component may even become dominant in the power flow. Therefore, at frequencies $ka > 1$, this component should be included into the source model together with the monopole component. But the quadrupole and higher harmonics can be neglected, as follows from Fig. 9, up to frequency $ka = 4$. At frequencies higher than this, the quadrupole component may be comparable with others or even dominant. The quadrupole component should thus be taken into account in the source model in the frequency range $ka > 4$. The next (octupole, $n = 3$) component should be taken into account in the range $ka > 5$, etc.

Thus, from the analysis of the free space pressure it follows that one should retain in the source model of Example 1 a single harmonic at frequencies $ka < 1$, two harmonics in the low- and mid-frequency range, up to $ka < 4$, and three harmonics in the range up to $ka < 5$, etc. Having done this, the harmonics not included in the model may give noticeable contribution only at some discrete frequencies. Such a choice of the optimal number of harmonics is in a good agreement with the choice based on comparison against the exact solution—see Fig. 7 as well as Fig. 10 where the contribution of harmonics to the radiated power is shown along with the exact value of the power flow.

The authors believe that the optimal number of essential harmonics can be estimated by using this simplified procedure for real noise sources too. Note that the free space pressure of the source under study is available from experimental identification of the model parameters, Section 3,

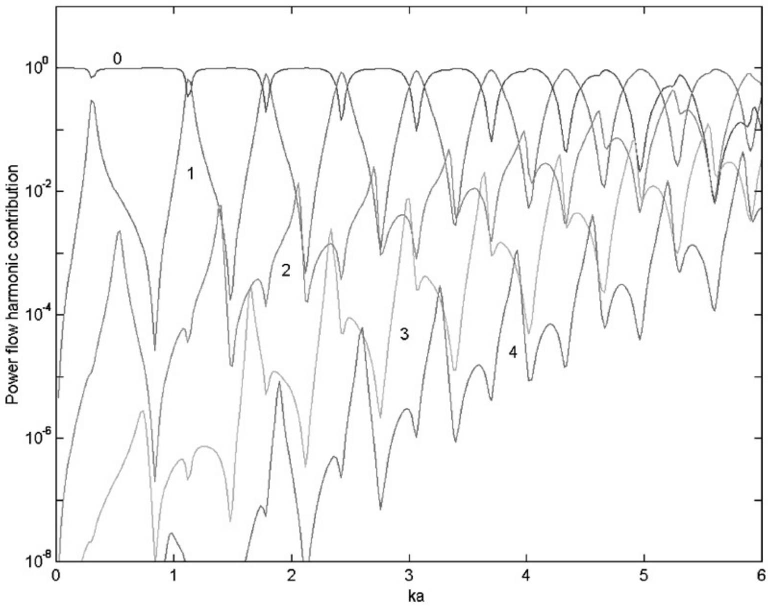

Fig. 10. Relative contribution of spherical harmonics $n = 0-4$ into the total power flow (25) in Example 1.

while the values of the loss factor for many rooms of the industrial type are documented or can be readily estimated [32].

A little different situation takes place when the blocked pressure is available instead of the free space pressure. Since the blocked pressure is measured in a cavity bounded by a closed acoustically rigid control surface S, it is strongly affected by the resonances of the cavity. Some of the amplitudes of the spherical harmonics will be amplified by the resonance while others reduced by antiresonance. Though this change of amplitudes should not affect the final results of prediction—see Eq. (6), this makes it difficult to extract the essential harmonics from the measured blocked pressure and to cut off insignificant harmonics. For illustration, Fig. 11 shows the relative amplitudes of spherical harmonics (30) of the blocked pressure in Example 1. At frequencies below the first eigenfrequency of the blocked cavity, which corresponds to the first root of equation $j_1'(ka) = 0$ equal to $ka = 2.07$, the relations between the amplitudes are similar to those for the free space amplitudes shown in Fig. 9. However at higher frequencies, $ka > 1.5$, the relations are strongly influenced by the resonances of the blocked cavity. For example, in a vicinity of frequency $ka = 3.34$, which is a root of the equation $j_2'(ka) = 0$, the quadrupole harmonic ($n = 2$) becomes dominant in the blocked pressure. At the same time, there is no increase in the free space pressure (see Fig. 9), nor in the coupled acoustic field of the chamber (see Fig. 7). Moreover, as follows from Fig. 10, at these frequencies the quadrupole component can be even neglected. Similarly, in the vicinity of frequency $ka = 4.5$ the components $n = 1, 2$ seem insignificant though in reality this is not so—see Fig. 10. The reason is that the zeroth and third harmonics have resonance frequencies in this region ($ka = 4.49$ is a root of $j_0'(ka) = 0$ and $ka = 4.52$ a root of $j_3'(ka) = 0$). Therefore, amplitudes of the zeroth and third harmonics are amplified

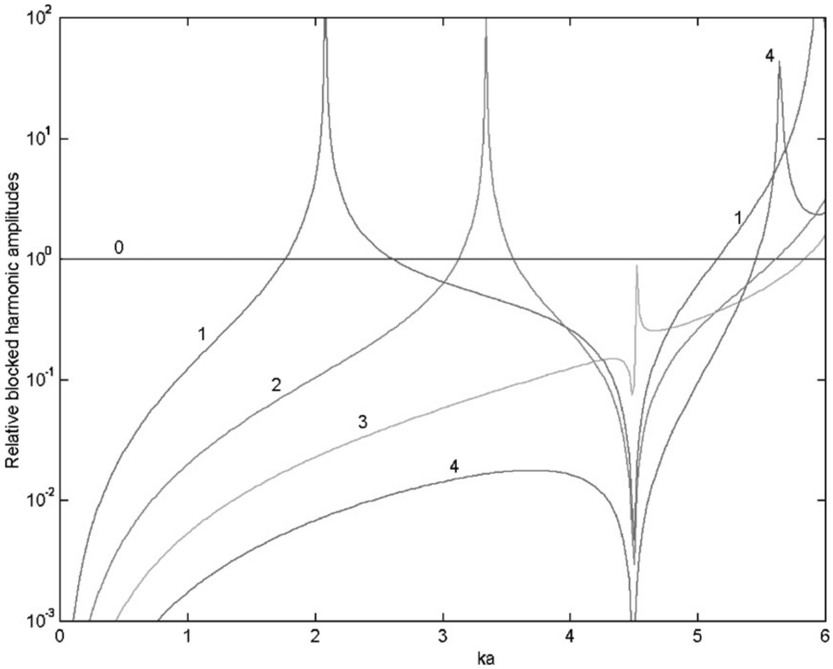

Fig. 11. The blocked pressure spherical harmonic amplitudes (30), normalized with the amplitude of the zeroth harmonic, for orders $n = 0-4$.

while the amplitudes of the first and second harmonics become relatively small, though they contribute a lot to the total power (Fig. 10).

It can be concluded that the optimal number of essential harmonics of the source model can be determined directly from the measured blocked pressure at frequencies below the minimum eigenfrequency $(ka)_{min}$ of the blocked cavity, e.g., at frequencies $ka < 0.7(ka)_{min}$: in Example 1, $ka < 1.5$. However, this becomes impossible when the frequency range of interest comprises eigenfrequencies of the blocked cavity as depicted, e.g., in Fig. 11. Perhaps, the best way to overcome the difficulty in this case is to compute the free space pressure vector via the blocked pressure vector in Eq. (10) and then execute the procedure described above.

Concerning the choice of an appropriate size of the control surface S, the general requirement is that it should envelop the source and be inscribed in the room. From the point of view of minimizing the number of essential harmonics on S, larger surfaces are more preferable: high order harmonics are poor radiators and their acoustic fields decay fast with the distance from the source [29]. On the other hand, smaller surfaces are more convenient for measurement. So in practice, there exists an optimal size of the control surface.

One more remark is appropriate at this point. The position of a source inside the control surface should be as symmetric as possible. Any eccentricity may unjustifiably increase the number of essential harmonics in the source model. This is evident, e.g., from Eq. (21) of Example 1: the amplitude of the nth spherical harmonic on S is proportional to $j_n(kl)$ and, hence, increases with the eccentricity l as l^n (for $kl \ll 1$). As the source geometry is, as a rule, not symmetric, the requirement on symmetry applies in fact to the radiation pattern created by the source. Thus proper positioning of the source within the test room may require first finding its radiation pattern and then adjusting the physical position of the source in relation to it.

6. Source characterization

The notions "modelling" and "characterization" of noise sources are not defined accurately. Some consider them synonyms, some not. The authors of the present paper distinguish between the two terms. Modelling is understood here as such a simplified description of a sound source that allows one to *predict* the sound field of the source in various acoustic environments. Source characterization is understood as a simplified description aiming at *comparison* of different sources with respect to noise generation potential.

Though the source model presented in this paper contains the minimal number of parameters necessary for prediction, they are too numerous for noise source characterization. For example, when the number of essential spherical harmonics is equal to $N = 4$ or 5, the total number of the model parameters is 10 or 15. It is difficult to compare two different noise sources each having such a number of parameters. Therefore, for characterization purposes, it is desirable to reduce the number of model parameters combining them into a new physically meaningful characteristic or descriptor which reflects the ability of a machine or other industrial product to produce noise, independently of the acoustic load. Several candidates for such a descriptor are considered below.

The sound power is a very attractive and commonly used descriptor of a noise source [33]. Unfortunately, it depends not only on the source parameters but, equally, on the parameters of the acoustic load. For various acoustic environments the sound power may vary from zero, when the source is loaded by a pure reactive impedance, to the maximum value

$$W_{max} = \tfrac{1}{8}\boldsymbol{b}^*(\mathrm{Re}\,\boldsymbol{Z_S})^{-1}\boldsymbol{b}, \tag{43}$$

which corresponds to the particular acoustic load compensating the source reactance, i.e., the imaginary part of the source impedance, $\mathrm{Im}(\boldsymbol{Z_S} + \boldsymbol{Z_L}) = 0$, while having the resistance equal to that of the source, $\mathrm{Re}\,\boldsymbol{Z_L} = \mathrm{Re}\,\boldsymbol{Z_S}$. The limiting value of the sound power (43) depends only on the source parameters and can therefore be considered as the sought descriptor of a noise source.

Another possibility is to use the sound power in a prescribed or standardized acoustic environment for characterization, e.g., in free space. Since the impedance matrix $\boldsymbol{Z}_\infty$ of the free space is available, Eq. (9), this descriptor is computed via the source parameters as

$$W_\infty = \tfrac{1}{2}\boldsymbol{b}^*(\boldsymbol{Z}_S^* + \boldsymbol{Z}_\infty^*)^{-1}\mathrm{Re}\,\boldsymbol{Z}_\infty(\boldsymbol{Z_S} + \boldsymbol{Z}_\infty)^{-1}\boldsymbol{b} = \tfrac{1}{2}\boldsymbol{p}_\infty^*\,\mathrm{Re}\,\boldsymbol{Y}_\infty\boldsymbol{p}_\infty. \tag{44}$$

Other acoustic environments are also possible, e.g., a half-space over a rigid plane boundary.

A sound source may also be characterized by its free space pressure vector normalized with the fluid impedance ρc to give a power-like descriptor

$$W_0 = \boldsymbol{p}_\infty^*\boldsymbol{p}_\infty/2\rho c. \tag{45}$$

Any of the quantities (43)–(45) can serve for characterization of sound sources. It should be realized, however, that if, say, a source 1 has a lower value of descriptor (45) than a source 2, $(W_0)_1 < (W_0)_2$, this does not imply that such a ranking will hold in all environments. There always exists a room in which the sound power (8) of source 1 is greater than that of source 2. This is valid also for descriptors (43), (44) and for any other possible source descriptors. The actual sound power (8) depends on many parameters and, therefore, cannot be adequately described by one descriptor. So, it can be stated that there does not exist a single descriptor which can fully characterize a sound source independently of its environment.

This pessimistic statement, however, does not exclude usefulness of quantities (43)–(45) or similar descriptors for source characterization. Practically, for each category of industrial noise sources, a category of their possible acoustic environments can be identified. One typical "average" environment can be taken as "the standard acoustic environment" and the sound power in this environment can be used for the characterization of noise sources from the same category. But this point requires more study.

7. Conclusions

A new model of an arbitrary airborne noise source is developed in this paper. It can be used for noise prediction in complex environment conditions. The model, described by a limited number of parameters—the source impedances and blocked pressure, is invariant with respect to the surrounding acoustical environment.

Procedures for experimental identification of model parameters in an arbitrary enclosure are presented. These procedures require only conventional equipment and facilities, thus can be potentially applied widely. Two simple examples have confirmed the validity of the approach.

Acknowledgements

The work was partly supported by the Russian Foundation for Basic Research (grant 00-01-00577a).

References

[1] A.P. Dowling, J.E. Ffowcs Williams, Sound and Sources of Sound, Ellis Horwood, London, 1983.
[2] A.D. Jones, Modelling the exhaust noise radiated from reciprocating internal combustion engines—a literature review, Noise Control Engineering 23 (1984) 12–31.
[3] R.H. Lyon, R.G. De Jong, Statistical Energy Analysis, Second Edition, Butterworth-Heinemann, Boston, 1995.
[4] L.D. Landau, E.M. Lifshitz, Hydrodynamics, Nauka, Moscow, 1986 (in Russian).
[5] E.G. Williams, J.D. Maynard, E. Skudrzyk, Sound source reconstruction using a microphone array, Journal of the Acoustical Society of America 68 (1980) 340–344.
[6] T. Loyau, J.-C. Pascal, P. Gaillard, Broadband acoustic holography reconstruction from acoustic intensity measurements, Journal of the Acoustical Society of America 84 (1988) 1744–1750.
[7] J. Hald, Spatial transformation of sound fields (STSF) techniques in the automotive industry, Brüel & Kjær Technical Review 1 (1995) 3–36.
[8] P.W. Partridge, C.A. Brebbia, L.C. Wrobel, The Dual Reciprocity Boundary Element Method, Elsevier Applied Science, London, 1992.
[9] I-DEAS, Master Series, Manual de References, Structural Dynamics Research Corporation, Milford, OH, 1996.
[10] Numerical integration technologies, SYSNOISE, The Revision 5.2, Reference Manuel, N.V. Leuven, Belgium, 1995.

[11] N.D. Perreira, S. Dubovsky, Analytical method to predict noise radiation from vibrating machine systems, Journal of the Acoustical Society of America 67 (1980) 551–563.
[12] G.H. Koopmann, H. Benner, Method for computing the sound power of machines based on Helmholtz integral, Journal of the Acoustical Society of America 71 (1982) 78–89.
[13] J.K. Jiang, M.G. Prasad, A parametric study of acoustical fields of vibrating structures for noise control applications, Journal of the Acoustical Society of America 83 (1988) 1420–1430.
[14] W. Williams, N.G. Parke, D.A. Moran, C.M. Sherman, Acoustic radiation from a finite cylinder, Journal of the Acoustical Society of America 36 (1964) 2316–2322.
[15] Yu.I. Bobrovnitskii, T.M. Tomilina, Calculation of radiation from finite elastic bodies by method of equivalent sources, Soviet Physics Acoustics 36 (1990) 334–338.
[16] G. Pavic, Acoustic source characterisation using an inverse procedure, Proceedings of the Eighth International Congress on Sound and Vibration, Hong Kong, China, 5-8 July, 2001, pp. 1623–1628.
[17] L.M. Chen, D.G. Schweikert, Sound radiation from arbitrary body, Journal of the Acoustical Society of America 35 (1963) 1626–1632.
[18] E. Luzzato, C. Lecointre, Some simple and effective methods for sound source identification with geometrical acoustic models, Journal of Sound and Vibration 105 (1986) 473–490.
[19] M. Jessel, Acoustique Theorique, Masson, Paris, 1973 (in French).
[20] P.J.T. Filippi, D. Habault, J. Piraux, Noise source modelling and intensimetry using antenna measurement and identification procedures, Journal of Sound and Vibration 124 (1988) 285–296.
[21] Yu.I. Bobrovnitskii, Acoustic modelling of machines, Soviet Physics Doklady 35 (1990) 937–939.
[22] Yu.I. Bobrovnitskii, K.I. Mal'tsev, N.M. Ostapishin, S.N. Panov, Acoustical model of a machine, Soviet Physics Acoustics 37 (1991) 570–574.
[23] M.L. Munjal, Acoustics of Ducts and Mufflers, Wiley, New York, 1987.
[24] R. Singh, W. Soedel, A review of compressor line pulsation analysis and muffler design research, 1974, Proceedings of the Purdue Compressor Technology Conference, Purdue University, USA, pp. 102–123.
[25] H. Bodén, The multi-load method for measuring the source characteristics of time-variant sources, Journal of Sound and Vibration 148 (1991) 437–453.
[26] Yu.I. Bobrovnitskii, Models of acoustical sources: a survey, Proceedings of Inter-Noise 2001, The Hague, Netherlands, 2001, pp. 3–6.
[27] Yu.I. Bobrovnitskii, A theorem on representation of the field of forced vibrations of a composite elastic system, Acoustical Physics 47 (2001) 409–411.
[28] D. Kupradze, Potential Methods in the Theory of Elasticity, IPFST, Jerusalem, 1965.
[29] E. Skudrzyk, Foundations of Acoustics, McGraw Hill, New York, 1971.
[30] L. Cremer, M. Heckl, E.E. Ungar, Structure-Borne Sound, Springer, Berlin, 1973.
[31] T.M. Tomilina, Yu.I. Bobrovnitskii, V.B. Yashkin, A.A. Kochkin, Power output of noise sources operating near elastic scatterers of finite dimensions, Journal of Sound and Vibration 226 (1999) 285–304.
[32] G.L. Osipov, E.Ya. Yudin (Eds.), Noise Control in Buildings and Urban Areas, Stroizdat, Moscow, 1987, 560pp. (in Russian).
[33] ISO 9614 – 1 Acoustics—Determination of Sound Power Levels of Noise Sources using Sound Intensity—Part 1: Measurement at Discrete Points, International Organisation for Standardisation. Geneva, Switzerland, 1993.